arXiv:1609.09156v1 [cs.CV] 28 Sep 2016

Similarity Mapping with Enhanced Siamese Network for Multi-Object Tracking

Minyoung Kim*
Panasonic Silicon Valley Laboratory
Cupertino, CA
minyoung.kim@us.panasonoic.com

Stefano Alletto
University of Modena and Reggio Emilia
Modena, MO
stefano.alletto@unimore.it

Luca Rigazio
Panasonic Silicon Valley Laboratory
Cupertino, CA
luca.rigazio@us.panasonic.com

Abstract

Multi-object tracking has recently become an important area of computer vision, especially for Advanced Driver Assistance Systems (ADAS). Despite growing attention, achieving high performance tracking is still challenging, with state-of-the-art systems resulting in high complexity with a large number of hyper parameters. In this paper, we focus on reducing overall system complexity and the number hyper parameters that need to be tuned to a specific environment. We introduce a novel tracking system based on similarity mapping by Enhanced Siamese Neural Network (ESNN), which accounts for both appearance and geometric information, and is trainable end-to-end. Our system achieves competitive performance in both speed and accuracy on MOT16 challenge, compared to known state-of-the-art methods.

1 Introduction

Object tracking has been evolving rapidly, becoming a very active area of research in machine vision. Several approaches have been proposed to improve tracking performance [1], with various applications from surveillance systems [2] to autonomous driving [3], and even sports analytics [4]. One major limitation of object tracking today, is the large number of hyper parameters required; this may harm robustness especially for real applications in unconstrained environments.

During the past few years, deep neural networks (DNNs) have become popular for their capability to learn rich features. Accordingly, new approaches with DNNs for tracking have also been proposed [5–7]. These methods take advantage of Recurrent Neural Networks (RNNs) to incorporate temporal information. Although some of these methods outperform conventional ones, computational requirements are high, resulting in very low frame rates and latency. Nevertheless, temporal information such as motion flow is crucial in object tracking, therefore cannot be discarded from a model without loss of performance.

To address these issues, we present a new high speed tracking system, combining both appearance and temporal geometric information, while having a smaller number of hyper parameters. We achieve this by leveraging our newly designed Enhanced Siamese Neural Network (ESNN) architecture for similarity mapping: the ESNN is an extended Siamese neural network that combines appearance

*This paper is the main project of the first author at Panasonic Lab.

11th Women in Machine Learning Workshop (WiML 2016), colocated with NIPS 2016, Barcelona, Spain.

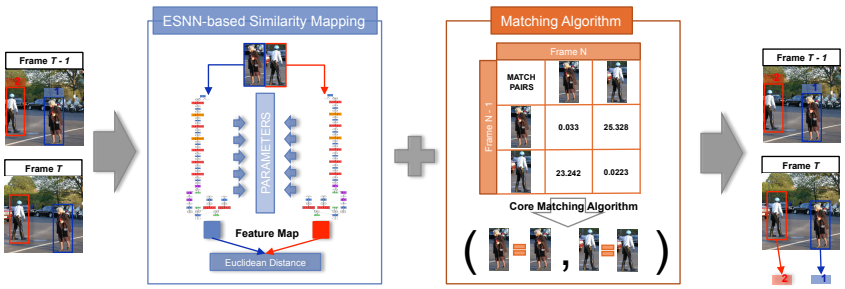

Figure 1: ESNN-based Multi-Object Tracking System

similarity with temporal geometric information and efficiently learns both visual and geometric features during end-to-end training. The rest of our paper is organized as follows: Section 2 describes available benchmark suits and our system overview. In Section 3, we describe architectures of the Base Network and ESNN along with training process and results comparison, and a simple yet efficient matching algorithm in Section 4. We evaluate the system in Section 5, and conclude in Section 6.

2 Background

Although multiple object tracking plays a key role in computer vision with help from new datasets for visual tracking coming out every year, there exist few benchmarks for pedestrian tracking, fewer than for object detection [3, 8–10]. One reason is the difficulty in standardizing the evaluation protocol, a controversial topic this day [11]; another reason may be high cost annotation. MOT16 [12] and KITTI tracking benchmarks [3] provide well established evaluation protocol with good quality of annotations, and are being widely used by researchers. MOT16 consists of 14 different sequences and KITTI consists of 50 sequences. Whereas KITTI videos are taken with moving cameras (attached to a vehicle), MOT sequences are taken with both static and moving ones. Also, even though both of datasets contain multiple objects types such as cars, cyclists, pedestrians, and motorbikes, KITTI evaluates only on cars and pedestrians and MOT16 evaluates only pedestrians. For fair comparison, MOT16 evaluation specifies additional information used by each submitted methods, for example, whether a method is online (no latency), and is using provided detection results.

In this paper, we propose an online system, based on provided detection results for two main reasons: first, we focus on visual tracking for ADAS and autonomous driving, and we believe reliable/low-latency tracking system is crucial. Secondly, since detection performance highly affects tracking quality, and we want to focus our efforts on improving the tracking algorithm, we choose to use provided detection results for fair comparison. Fig. 1 illustrates our tracking system based on ESNN. The system can be divided into two procedures; 1) ESNN-based Similarity Mapping and 2) Matching. A Siamese network, referred to as 'Base Network', is pre-trained with visual information of objects. Then, ESNN takes Intersection-over-Union (IoU) and Area Ratio information from pairs of objects as additional features, and builds a combined similarity mapping with both geometric and pre-trained Siamese network features. After ESNN is fully trained and similarity scores are computed, the matching algorithm produces final tracking results.

3 Similarity Mapping

ESNN uses a Siamese neural network that consists of two identical sets of convolutional neural networks, where the weights of convolution layers are shared in between. The network takes a pair of image patches, cropped from original frame, and then maps them to $L2$ space where the Euclidean distance between each output can be used as similarity scores. The Base Network is built and trained first, then is extended to ESNN with geometric information.

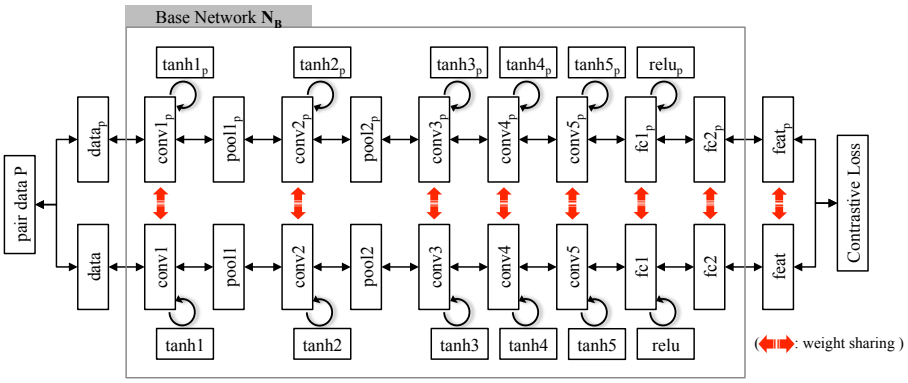

Figure 2: Architecture of Base Siamese Neural Network for Similarity Training

3.1 Architecture

3.1.1 Base Network Architecture

The base architecture of our Siamese neural network is described in Fig. 2. For each convolution layer, *hyperbolic tangent* (*TanH*) is used as activation function, and the first fully connected layer is followed by *Rectified Linear Unit* (*ReLU*) [13]. Kernel size for each convolution and pooling layer is as follows: conv1(5x5), pool1(2x2), conv2(3x3), pool2(2x2), conv3(3x3), conv4(2x2), conv5(2x2), fc1(2048), fc2(1024), and feat(2) or feat(4). The feat(2) layer is fine-tuned with the new feat(4) layer to incorporate geometrical features in ESNN. For loss function, contrastive loss L_c, proposed in [14], is used as follows:

$$E_n = \|F - F_p\|_2 \tag{1}$$

$$L_c = \frac{1}{2N}\sum_{n=1}^{N}(y)E_n^2 + (1-y)\max(m - E_n, 0)^2 \tag{2}$$

where E_n is Euclidean distance between the output features F and F_p of the Siamese neural network with input data pair d and d_p, shown in Fig. 2. y denotes label of the pair, where $y = 1$ if (d, d_p) is a matching pair and $y = 0$ otherwise. Finally, m is a margin parameter that affects contribution of non-matching pairs to the loss L_c, and we choose $m = 3$ as the best margin obtained by experiments.

3.1.2 ESNN Architecture

In extension of the Base Network architecture above, the ESNN takes additional layers that learn from IoU D_{iou}, and area variant of a pair of objects D_{Arat}. For a pair of object bounding boxes b_i and b_j, appearing in frame f_{t-1} and f_t, D_{IoU} and D_{Arat} are calculated as follows:

$$[D_{IoU}, D_{Arat}](b_i, b_j) = [\frac{area(b_i \cap b_j)}{area(b_i \cup b_j)}, \frac{min(area(b_i), area(b_j))}{max(area(b_i), area(b_j))}] \tag{3}$$

Fig. 3 shows the extended architecture of our network. The additional layers up-sample input to the same dimension as the output of the Base Network N_B, $feat$ and $feat_p$. Layers in N_B are locked during the first phase of training.

3.2 Dataset

3.2.1 Market-1501

Market-1501 person re-identification dataset [15], which is used for initial training, contains 1,501 identities with annotation available for both train and test sets. Market-1501 is collected by 6 cameras from different angles, compared to MOT16 dataset where video sequences are taken from a single-view point (although each sequence is taken from different view point, e.g. camera attached to a car, hand-held camera, etc). It becomes more challenging, but certainly provides various features for

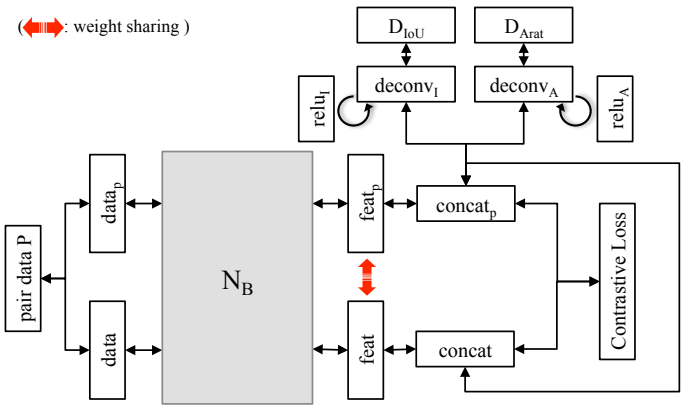

Figure 3: Architecture of Enhanced Siamese Neural Network

a unique identity that helps neural network parameters learn well enough to be generalized. From Market-1501, training patches for the Base Network are generated by randomly selecting matching and non-matching pairs among different persons. Each pair has size of 128(w)x128(h), occupying 64(w)x128(h) for each person. Labels are produced depending on IDs; 1 for matching pair and 0 for non-matching pair. 75,000 matching and 75,000 non-matching pairs are generated for training, and 25,000 each for testing set.

3.2.2 MOT16

Once the first model is obtained by using Market-1501, MOT16 dataset that consists of 7 train and 7 test sequences is used to fine-tune both the Base Network and ESNN. The train sequences (MOT16-02, 04, 05, 09, 10, 11, and 13) contain 79,790 detections, and testing sequences (MOT16-01, 03, 06, 07, 08, 12, and 14) contain 135,376 detections of pedestrians. As the test sequences don't have groundtruth information, train sequences are split into train and validation set, 6 sequences for the train set, and 1 sequence for validation. Matching and non-matching pairs from two sequential frames are generated, along with IoU and AreaRatio data, calculated by Eq. 3. In total, around 222,400 samples are generated for train set, and 198,800 samples for validation set. We set *1:4* to *1:6* ratio between the number of matching and non-matching pairs.

3.3 Training

The Base Network is pre-trained on Market-1501 first. With batch size of 128, learning rate starting from 0.01, and SGD (Stochastic Gradient Descent), our Siamese neural network converges well on pairs generated by Market-1501 dataset. Train and test losses of the training are shown in Fig. 4 (*left*). *x-axis* represents the number of epochs in two different scale for each loss. On Market-1501 test set, the trained model achieves $precision = 0.9854$, $recall = 0.9774$, and $F_1 = 0.9814$ where F_1 score is calculated by the function as follows:

$$F_1 = \frac{2TP}{2TP + FP + FN} \tag{4}$$

where TP is # of True Positives, FP is # of False Positives, and FN is # of False Negatives. Also, Fig. 4 (*right*) shows the Euclidean distance of the data pairs, generated from the trained model on Market-1501 test set in logarithm scale (*y-axis*). With this pre-trained model, the network is then fine-tuned on MOT16 dataset. Results will be discussed at the end of this section along with ESNN training results.

To train ESNN, the pre-trained Base Network model parameters are transferred. In fine-tuning, layers in the Base Network are locked in the beginning, and unlocked in the final phase. Also, margin is set to $m = 0.5$. Once the ESNN model is obtained, we analyze it both on train and validation set, and compare the performance with results from the Base Network. Fig. 5 and Fig. 6 show the Euclidean distance of MOT validation and train set from the Base Network (*left*) and ESNN (*right*). On each figure, the plot on top represents the Euclidean distance (*y-axis*) with IoU (*x-axis*) of the data. The bottom plot shows histogram of the Euclidean distance (*x-axis*) with normalized frequency (*y-axis*).

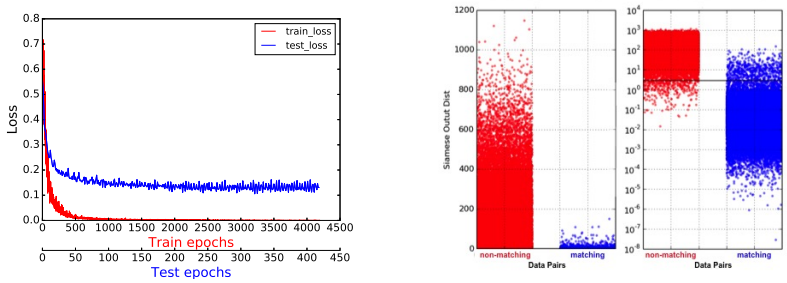

Figure 4: Train/Test Loss of the Base Network (*left*) and Euclidean distance of Market-1501 test set with margin, $m = 3$ (black horizental line) (*right*)

The red points represent non-matching pairs, blue points for matching pairs, and red and blue dashed lines represent mean distance of each group. Finally, black dashed line represents margin m.

The Base Network model achieves $precision = 0.9837$, $recall = 0.9966$, and $F_1 = 0.9901$, and the ESNN model achieves *precision=0.9908*, *recall=0.9990*, and $F_1 = 0.9949$ on validation set. Also, it turns out that the validation set, which we selected 1 sequence from MOT16 train data, is distinctive from others, because IoU is discriminative enough for matching and non-matching pairs. Both figures show that the ESNN model outperforms the Base model. Note that, some of the misclassified non-matching pairs with $D_{IoU} < 0.05$ by the Base Network model are correctly classified by the ESNN model. It means the ESNN can handle the object pairs, far apart but sharing similar features (e.g. two far-aparted persons with similar clothing), better than the Base Network by utilizing IoU and area variant information.

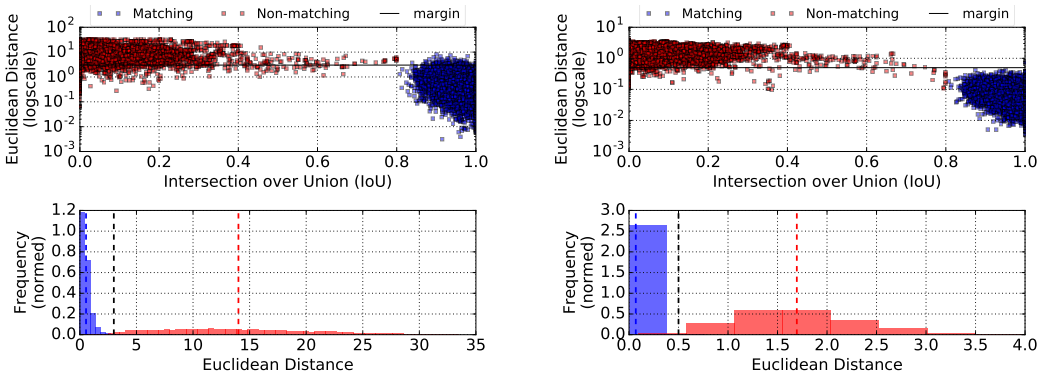

(a) Base Network Model

(b) ESNN Model

Figure 5: Euclidean Distance on MOT16 Validation Set

4 Matching Algorithm

For the Base Network, a new score function is introduced by taking IoU and area variant in account, plus the score from Euclidean distance. For the ESNN, only Euclidean distance is used for scoring.

4.1 Scoring

Given detection boxes $B_{t-1} = \{b_1, \ldots, b_n\}$ at frame $t-1$, and $B_t = \{b_1, \ldots, b_m\}$ at frame t, new score function for a pair $S_{New}(b_i, b_j)$ where $b_i \in B_{t-1}, \forall i = 1, \ldots, n$, and $b_j \in B_t, \forall j = 1, \ldots, k$, can be derived as follows:

$$S_{New} = S_{Dist} + S_{IoU} S_{Arat} \tag{5}$$

where S_{Dist} denotes the score derived from the Euclidean distance $D_{siam}(b_i, b_j)$, output of our network for the pair (b_i, b_j), S_{IoU} denotes Intersection-over-Union of the pair, shifted by 1.0, and

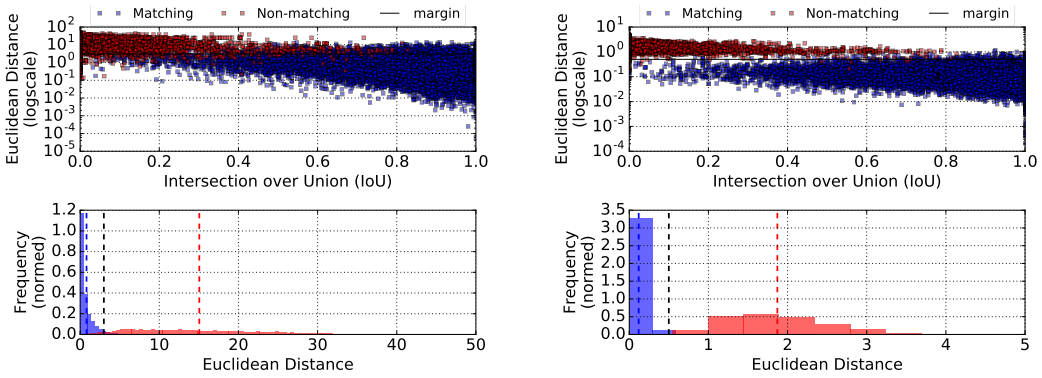

(a) Base Network Model

(b) ESNN Model

Figure 6: Euclidean Distance on MOT16 Train Set

S_{Arat} denotes the ratio of area between them. To shorten notation, $S(b_i, b_j)$ is written as S in Eq. 5. The exact functions of S_{Dist}, S_{IoU}, and S_{Arat} are:

$$S_{Dist}(b_i, b_j) = \alpha \log_{0.1}\{max(\gamma, D_{siam}(b_i, b_j))\} \tag{6}$$

$$S_{IoU}(b_i, b_j) = 1.0 + \frac{area(b_i \cap b_j)}{area(b_i \cup b_j)} \tag{7}$$

$$S_{Arat}(b_i, b_j) = e^{\frac{min(area(b_i), area(b_j))}{max(area(b_i), area(b_j))} - \delta} \tag{8}$$

where we choose $\alpha = 0.8$, $\gamma = 10^{-5}$, and $\delta = 0.2$ as a bias term. Finally, S_{New} is obtained for the Base Network model, and S_{Dist} for the ESNN model.

$$S_{Net} = \begin{cases} S_{New}, & \text{if } Net = N_B \\ S_{Dist}, & \text{otherwise} \end{cases} \tag{9}$$

4.2 Matching

As the second part of the tracking system, a simple yet efficient matching algorithm that takes the score matrix S_{Net} as an input is derived as shown in Algorithm. 1. Only one hyper parameter is introduced by the algorithm, denoted by f_n, specifying how many frames the tracker looks back to generate pairs with the current frame. With f_n and S_{Net} map where data pair P is the keys, the algorithm starts matching with the highest similarity score. It returns the best match solely based on the scores, and when there is a conflict, it tries once more to find a better match which can be replaced with the current match. After all possible pairs are examined and redundant pairs are filtered, new IDs are assigned to the leftover targets.

To provide a deeper insight on the advantages of this algorithm, we also employ a matcher based on the popular Hungarian algorithm and report the obtained results in the experimental section. One of the major differences between our proposed matching strategy and the Hungarian algorithm is computational complexity. In fact, while the former runs in linear time with the number of people in the scene, the Hungarian algorithm has a complexity of $O(n^3)$ and can become a significant performance bottleneck in crowded sequences.

5 Evaluation

Our system is evaluated on MOT16 train and test set. Table 1 shows evaluation results on the training set, and the highest MOT Accuracy ($MOTA$) comes from MOT16-09 sequence, whereas MOT16-13, known to be the hardest sequence, yields the lowest $MOTA$, resulting in average $MOTA = 30.2$. Running time differs from sequences, because it depends on the density of the sequence, that the more number of detections on frames, the more computation for both forward propagation of the Siamese network with more possible pairs, and matching algorithm need. The speed benchmark is

Algorithm 1 Matching Algorithm

procedure MATCH(P, f_n) ▷ Score matrix as input
  $exID \leftarrow$ {*existing IDs whithin previous n frames*}
  for i *in* $reversed(sorted(P, score))$ **do** ▷ *sort pairs with score*
    $(ID_{exist}, ID_{tgt}) \leftarrow P[i]$ ▷ *pull candidate pair*
    if $ID_{tgt} \notin exID$ **then**
      continue
    end if
    if $ID_{tgt}.notAssigned()$ **then**
      if $ID_{exist}.notAssigned()$ **then**
        $Target[ID_{exist}] \leftarrow ID_{tgt}$ ▷ *new assignment*
        $ID_{exist}.setAssigned(True)$
      else if $newID_{exist} \leftarrow FindBetterMatch()$ **then**
        $ID_{exist}.setAssigned(False)$
        $Target[newID_{exist}] \leftarrow ID_{tgt}$ ▷ *switch assignment*
        $newID_{exist}.setAssigned(True)$
      end if
    end if
  end for
  for $ID_{tgt} \in$ {*leftover tgt IDs*} **do**
    $exID.append(ID_{tgt}, f_{new})$ ▷ *handle new IDs with frame info*
  end for
end procedure

conducted by using NVIDIA GeForce GTX 1080 card. The results on test set is shown in Table 2, along with other methods for comparison. Only the referencible methods that use provided detection results are shown, along with an indication whether the method is online or not.

Even though the accurate comparison on speed is not quite possible, due to lack of information on hardware specification where other benchmarks were conducted, the speed of our method is quite noticeable while achieving competitive performance. Table 2 also shows that our method tends to produce more number of track fragmentations, indicating that there is a room for improvement in matching algorithm, along with lessening score threshold. It also relates to the number of False Positives and False Negatives, that by the score threshold tuning, it is possible to compensate False Negatives which might reduce the possibility of losing the tracking and regain it.

Given the score matrix S_{Net} provided by the siamese network, we compare the performance of the proposed matching algorithm to a baseline that uses the widely adopted Hungarian algorithm, whose results are reported in Table 3. The proposed matching approach is generally better than the Hungarian algorithm, providing an increase in MOTA of 2.5 points. More in detail, it can be noticed that the Hungarian algorithm occasionally favors committing ID switches instead of fragmentations, e.g. in the sequences MOT16-04 (73% FM, 128% IDs), MOT16-11 (76%, 301% IDs), MOT16-13 (84%, 100% IDs). This is due to the algorithm assigning new IDs to detections in a bipartite graph matching fashion, which inherently leads to a more complete solution, albeit a lesser accurate one.

Furthermore, the high computational complexity of the Hungarian algorithm results in the matching algorithm being 1.91 times slower. While the execution time is substantially unchanged in some scenarios such as MOT16-05 (1.03 times slower), the Hungarian's poor scalability is especially clear when dealing with the most crowded scenes, e.g. MOT16-04 (2.69 times slower). On the other hand, the proposed matching solution scales linearly with the number of detections in the scene, resulting in better performance when the density of the sequence increases.

6 Conclusion

In this paper, we proposed a new approach for multiple object tracking system that takes advantage of deep Siamese neural network to model similarity mapping, followed by an efficient matching algorithm. We showed the capability of our Enhanced Siamese neural network, that can fuse appearance features with geometric information such as IoU and area variant of objects, resulting

Table 1: Benchmark Results on MOT16 Train Dataset

Name	MOTA	MOTP	MOTAL	Density	Hz	Rcll	Prcn	FAR	GT	MT	PT	ML	FP	FN	IDs	FM
MOT16-02	17.1	75.5	17.5	29.7	*19.70*	18.2	96.3	0.21	59	4	14	41	125	14590	75	255
MOT16-04	34.7	78.4	35.3	45.3	*7.20*	40.1	89.3	2.18	82	6	42	34	2286	28479	302	1185
MOT16-05	31.0	76.1	32.0	8.1	*46.53*	35.4	91.5	0.27	133	5	63	65	224	4407	74	206
MOT16-09	48.4	73.7	49.5	10.0	*22.24*	53.0	93.8	0.35	25	3	18	4	184	2469	60	151
MOT16-10	31.4	74.8	32.3	18.8	*26.88*	36.5	89.7	0.79	54	5	19	30	515	7825	111	453
MOT16-11	48.2	78.2	48.92	10.2	*26.22*	52.7	93.3	0.38	73	8	28	37	346	4337	66	147
MOT16-13	6.8	73.2	7.3	15.3	*37.60*	13.4	68.7	0.91	85	6	17	62	684	9716	56	172
TOTAL	30.2	77.0	30.8	20.8	*17.91*	34.8	89.8	0.82	511	37	201	273	4364	71823	744	2569

Table 2: Benchmark Results on MOT16 Test Dataset [16]

Method	Online	MOTA	MOTP	Hz	FAF	MT	ML	FP	FN	IDs	Frag
NMOT [17]	No	46.4	76.6	*2.6*	1.6	18.3%	41.4%	9,753	87,565	359	504
JMC [18]	No	46.3	75.7	*0.8*	1.1	15.5%	39.7%	6,373	90,914	657	1,114
MHT_DAM [19]	No	42.8	76.4	*0.8*	1.2	14.6%	49.0%	7,278	96.607	462	625
Ours	Yes	35.3	75.2	*7.9*	0.9	7.4%	51.1%	5,592	110,778	1,598	5,153
TBD [20]	No	33.7	76.5	*1.3*	1.0	7.2%	54.2%	5,804	112,587	2,418	2,252
CEM [21]	No	33.2	75.8	*0.3*	1.2	7.8%	54.4%	6,837	114,322	642	731
DP_NMS [22]	No	32.2	76.4	*212.6*	0.2	5.4%	62.1%	1,123	121,579	972	944
SMOT [23]	No	29.7	75.2	*0.2*	2.9	5.3%	47.7%	17,426	107,552	3,108	4,483
JPDA_m [24]	No	26.2	76.3	*22.2*	0.6	4.1%	67.5%	3,689	130,549	365	638

Table 3: Results on MOT16 Train Dataset obtained using the Hungarian algorithm as matching strategy

Name	MOTA	MOTP	MOTAL	Hz	Rcll	Prcn	FAR	GT	MT	PT	ML	FP	FN	IDs	FM
5 MOT16-02	14.9	75.2	16.0	*16.30*	19.1	86.1	0.92	59	4	14	41	549	14420	204	281
MOT16-04	30.4	78.5	31.2	*2.68*	35.9	88.4	2.14	82	6	40	36	2248	30481	388	871
MOT16-05	26.9	75.9	29.9	*45.10*	35.8	86.0	0.47	133	6	62	65	397	4379	207	205
MOT16-09	44.0	73.8	46.7	*18.01*	53.0	89.5	0.62	25	3	18	4	327	2473	142	157
MOT16-10	29.2	74.8	30.8	*22.36*	36.6	86.4	1.09	54	5	19	30	710	7814	201	456
MOT16-11	42.7	78.4	44.8	*23.18*	51.9	88.0	0.72	73	8	26	39	648	4410	199	113
MOT16-13	6.1	73.5	6.6	*35.51*	12.2	68.8	0.82	85	5	16	64	618	9855	56	146
TOTAL	27.7	75.7	29.4	*9.40*	34.9	84.7	0.97	511	37	195	279	5497	73832	1397	2229

in better performance while keeping no latency. Evaluation results show that using Siamese neural network has significant potential for building similarity matrices for multiple object tracking. Further research on optimizing the network architecture to reduce the numbers of network parameters can decrease run time, also augmenting data for training can help producing models with better performance.

References

[1] Li, X., Hu, W., Shen, C., Zhang, Z., Dick, A.R., van den Hengel, A.: A survey of appearance models in visual object tracking. CoRR **abs/1303.4803** (2013)

[2] Hu, W., Tan, T., Wang, L., Maybank, S.: A survey on visual surveillance of object motion and behaviors. Trans. Sys. Man Cyber Part C **34**(3) (August 2004) 334–352

[3] Geiger, A., Lenz, P., Urtasun, R.: Are we ready for autonomous driving? the kitti vision benchmark suite. In: Conference on Computer Vision and Pattern Recognition (CVPR). (2012)

[4] Wu, Y., Lim, J., Yang, M.H.: Online object tracking: A benchmark. In: IEEE Conference on Computer Vision and Pattern Recognition (CVPR). (2013)

[5] Gan, Q., Guo, Q., Zhang, Z., Cho, K.: First step toward model-free, anonymous object tracking with recurrent neural networks. CoRR **abs/1511.06425** (2015)

[6] Kahou, S.E., Michalski, V., Memisevic, R.: RATM: recurrent attentive tracking model. CoRR **abs/1510.08660** (2015)

[7] Ondruska, P., Posner, I.: Deep tracking: Seeing beyond seeing using recurrent neural networks. CoRR **abs/1602.00991** (2016)

[8] Dollar, P., Wojek, C., Schiele, B., Perona, P.: Pedestrian detection: An evaluation of the state of the art. IEEE Trans. Pattern Anal. Mach. Intell. **34**(4) (April 2012) 743–761

[9] Lin, T., Maire, M., Belongie, S.J., Bourdev, L.D., Girshick, R.B., Hays, J., Perona, P., Ramanan, D., Dollár, P., Zitnick, C.L.: Microsoft COCO: common objects in context. CoRR **abs/1405.0312** (2014)

[10] Russakovsky, O., Deng, J., Su, H., Krause, J., Satheesh, S., Ma, S., Huang, Z., Karpathy, A., Khosla, A., Bernstein, M., Berg, A.C., Fei-Fei, L.: ImageNet Large Scale Visual Recognition Challenge. International Journal of Computer Vision (IJCV) **115**(3) (2015) 211–252

[11] Luo, W., Zhao, X., Kim, T.: Multiple object tracking: A review. CoRR **abs/1409.7618** (2014)

[12] Milan, A., Leal-Taixé, L., Reid, I.D., Roth, S., Schindler, K.: MOT16: A benchmark for multi-object tracking. CoRR **abs/1603.00831** (2016)

[13] Hinton, G.E.: Rectified linear units improve restricted boltzmann machines vinod nair

[14] Hadsell, R., Chopra, S., Lecun, Y.: Dimensionality reduction by learning an invariant mapping. In: In Proc. Computer Vision and Pattern Recognition Conference (CVPR'06), IEEE Press (2006)

[15] Zheng, L., Shen, L., Tian, L., Wang, S., Wang, J., Tian, Q.: Scalable person re-identification: A benchmark. In: Computer Vision, IEEE International Conference on. (2015)

[16] : Multiple object tracking benchmark. `https://motchallenge.net/results/MOT16/`

[17] Choi, W.: Near-online multi-target tracking with aggregated local flow descriptor. CoRR **abs/1504.02340** (2015)

[18] Tang, S., Andres, B., Andriluka, M., Schiele, B.: Subgraph decomposition for multi-target tracking. In: CVPR, IEEE Computer Society (2015) 5033–5041

[19] Kim, C., Li, F., Ciptadi, A., Rehg, J.M.: Multiple hypothesis tracking revisited. In: Computer Vision (ICCV), IEEE International Conference on, IEEE (December 2015)

[20] Stiller, C., Urtasun, R., Wojek, C., Lauer, M., Geiger, A.: 3d traffic scene understanding from movable platforms. IEEE Transactions on Pattern Analysis and Machine Intelligence **36**(5) (2014) 1–1

[21] Milan, A., Roth, S., Schindler, K.: Continuous energy minimization for multitarget tracking. IEEE TPAMI **36**(1) (2014) 58–72

[22] Pirsiavash, H., Ramanan, D., Fowlkes, C.C.: Globally-optimal greedy algorithms for tracking a variable number of objects. In: Proceedings of the 2011 IEEE Conference on Computer Vision and Pattern Recognition. CVPR '11, Washington, DC, USA, IEEE Computer Society (2011) 1201–1208

[23] Dicle, C., Sznaier, M., Camps, O.: The way they move: Tracking targets with similar appearance. In: ICCV. (2013)

[24] Rezatofighi, S.H., Milan, A., Zhang, Z., Shi, Q., Dick, A., Reid, I.: Joint probabilistic data association revisited. In: ICCV. (2015)